Turkish Journal of Electrical Engineering & Computer Sciences

http://journals.tubitak.gov.tr/elektrik/

Research Article

Turk J Elec Eng & Comp Sci
(2017) 25: 4867 – 4879

doi:10.3906/elk-1703-122

ANN-based SHEPWM using a harmony search on a new multilevel inverter topology

Fayçal CHABNI*, Rachid TALEB, M'hamed HELAIMI
Department of Electrical Engineering, Faculty of Technology, Hassiba Benbouali University,
Laboratoire Génie Electrique et Energies Renouvelables (LGEER), Chlef, Algeria

Received: 10.03.2017 • **Accepted/Published Online:** 17.08.2017 • **Final Version:** 03.12.2017

Abstract: This article presents the application of the harmony search (HS) optimization algorithm for selective harmonic elimination PWM (SHEPWM) in a new topology of multilevel inverters with reduced number of electronic switching elements. The main objective of the harmonic elimination strategy is eliminating undesired low-rank harmonics in order to improve the quality of the output waveform. The harmonic elimination strategy is achieved by solving a system of nonlinear equations. In this paper harmony search optimization is applied using artificial neural networks (ANNs) on a new 21-level inverter topology. The algorithm is based on a music improvisation process. MATLAB programming software is used to develop a harmony search optimization program for harmonic elimination. A small-scale laboratory of the proposed 21-level inverter is built to validate the simulation results and to prove the efficiency of the proposed control scheme.

Key words: Multilevel inverter, harmonic elimination, harmony search, artificial neural network

1. Introduction

Direct current to alternating current (DC/AC) power conversion is a very important technology. Inverters play a critical role in machine drives, power transmission systems, induction heating, electric vehicles, and other technologies. The recent advancement in power electronic devices and the increasing demand on electrical energy have led to the development of multiple configurations of DC to AC converters.

The multilevel DC to AC cascade inverter is one of the most used topologies in high and medium power applications; the advantages provided by the cascade inverter such as higher output waveform quality than most inverter topologies and low voltage stress on the power switches make it a very attractive topology. In order to improve performance and reduce production cost, multiple studies such as [1] proposed new inverter architectures with reduced component count. In the present study a new multilevel inverter is proposed, using asymmetrical topology. The proposed inverter can generate 21 voltage levels with fewer switching devices compared to a conventional H-bridge cascade inverter; Figure 1 illustrates the generalized waveform generated by a 21-level inverter.

Sinusoidal and space vector modulation are two of the most commonly applied control strategies for multilevel DC to AC converters, but the main problem with these two techniques is the high switching frequency of the semiconductor devices, leading to high switching losses. A simpler yet efficient modulation method known as selective harmonic elimination can be used for the control of multilevel DC to AC converters. The method was

*Correspondence: chabni.fay@gmail.com

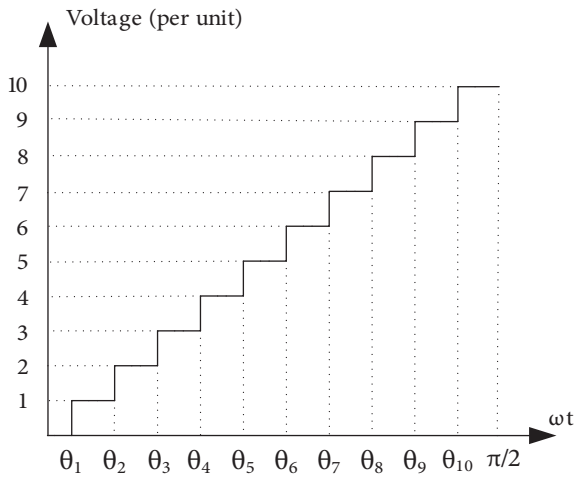

Figure 1. Quarter waveform of a 21-level inverter.

introduced for the first time in 1973 by Patel and Hoft in [2], and it was used to eliminate harmonics in single- and three-phase thyristor-controlled inverters. The method provides a lot of advantages such as eliminating low-rank harmonics and operating the switching devices at a low frequency, which leads to increasing the lifetime of switching components. However, the main problem with this method is the necessity of solving a set of nonlinear equations to determine the optimal switching angles that allow the elimination of low-rank harmonics.

Several numerical methods have been used to compute the optimal switching angles such as the theory of resultants and Newton–Raphson (N-R), but these methods are difficult to use especially when it comes to solving large number of equations. The N-R method requires an initial guess of the switching angles in such a way that they are close to the optimal values. Guessing the initial solutions of a set of nonlinear equations is extremely difficult especially for a large number of variables (switching angles).

Another approach to solve the optimal switching problem is using optimization algorithms, where the equations of SHEPWM are presented in a cost function that can be optimized. Multiple optimization methods were used for the SHEPWM problem such as firefly algorithm [3], differential evolution [4], genetic algorithms [5], and bat algorithm [6]. These methods allow the determination of the switching angles without an initial guess.

The harmony search (HS) is a new optimization algorithm inspired by the music improvisation process [7]. It was first introduced in 2001 by Geem in [8] and it was initially used to solve pipe network design problems in 2002 [9]. As a new population-based optimization algorithm the HS has drawn the attention of engineers and scientists all over the world and gained great success in multiple areas of research, especially in control and electrical power systems [10]. In this work the role of the HS algorithm is to solve the SHEPWM equations in order to determine the values of the optimal switching angles.

In recent years, artificial intelligence techniques such as artificial neural networks (ANNs) are used in power electronics and motor drive systems [11,12]; in this article ANNs are used to perform online control of the proposed multilevel inverter by deriving the switching angles corresponding to a given modulation index. The networks are trained offline with results obtained by the harmony search algorithm and later implemented to the control the targeted system (inverter).

The proposed new topology is presented in the second section. The third section explains briefly the SHEPWM strategy. Sections four and five present the harmony search optimization algorithm and the

application of neural networks for SHEPWM. Section six presents results obtained by computer simulation. The effectiveness of the *ANN*-harmony search based SHEPWM is verified in section seven using a small-scale laboratory prototype of the proposed multilevel inverter controlled by the STM32F407 microcontroller. This section also discusses the hardware implementation and experimental results.

2. Proposed CHB multilevel inverter

When compared to the flying capacitor and clamped diode configurations, the cascade H-bridge multilevel configuration offers a lot of advantages; however, the cascade configuration exhibits an important limitation for higher number of voltage levels. It requires a large number of switching devices, protection circuits, and heat sinks, thereby increasing production cost. A new topology is proposed in this work to overcome this problem by using nonequal DC input sources (also called asymmetric topology) and using a hybrid configuration of simple H-bridge topology and bidirectional switches in order to generate higher voltage levels with fewer switching devices than conventional topologies. Figure 2 shows the structure of the proposed 21-level inverter.

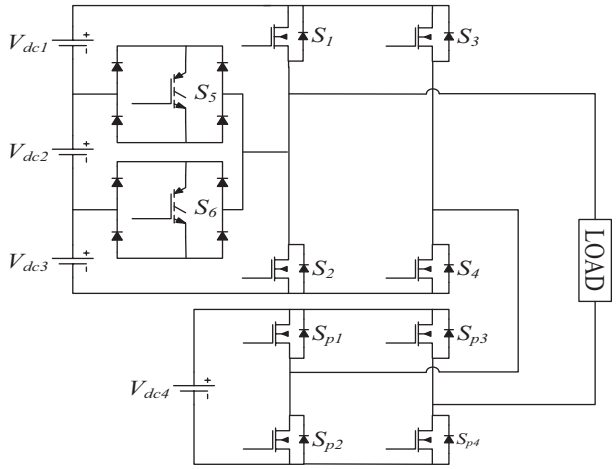

Figure 2. Structure of the proposed multilevel inverter.

The proposed 21-level single phase inverter is composed of two cells connected in series. The upper cell comprises a simple H-bridge formed by S_1, S_2, S_3, S_4 and two bidirectional switches S_5, S_6 and three DC sources with equal voltage values. The function of the bidirectional switches S_5 and S_6 is controlling the connection of the DC sources to construct the desired staircase output voltage waveform. The lower cell is a simple H-bridge formed by S_{p1}, S_{p2}, S_{p3}, and S_{p4}, connected to an isolated DC source.

The valid switching states for all possible combinations are presented in Table 1. It should be noted that these combinations are only valid for the following conditions:

$$V_{dc1} = V_{dc2} = V_{dc3} \tag{1}$$

$$V_{dc4} = 7 \times V_{dc1} \tag{2}$$

This means the voltage source connected to the second cell has to be seven times greater than a single voltage source used in the first cell in order to obtain 21 voltage levels. It can be seen from the proposed topology and Eq. (2) that the switching devices S_{p1}, S_{p2}, S_{p3}, and S_{p4} are under higher voltage stress comparing to the switching devices used in the upper bridge; therefore switching devices with high voltage rating must be used in the lower bridge.

Table 1. Output voltage levels ($p.u.$) with corresponding conducting switches.

Voltage (p.u.)	Switches in (ON) state	Voltage (p.u.)	Switches in (ON) state
10	S_1, S_4, S_{p1}, S_{p4}	–1	S_3, S_5, S_{p2}, S_{p4}
9	S_4, S_5, S_{p1}, S_{p4}	–2	S_3, S_6, S_{p2}, S_{p4}
8	S_4, S_6, S_{p1}, S_{p4}	–3	S_2, S_3, S_{p2}, S_{p4}
7	S_2, S_4, S_{p1}, S_{p4}	–4	S_1, S_4, S_{p2}, S_{p4}
6	S_3, S_5, S_{p1}, S_{p4}	–5	S_4, S_5, S_{p2}, S_{p4}
5	S_3, S_6, S_{p1}, S_{p4}	–6	S_4, S_6, S_{p2}, S_{p4}
4	S_2, S_3, S_{p1}, S_{p4}	–7	S_2, S_4, S_{p2}, S_{p4}
3	S_1, S_4, S_{p2}, S_{p4}	–8	S_3, S_5, S_{p2}, S_{p4}
2	S_4, S_5, S_{p2}, S_{p4}	–9	S_3, S_6, S_{p2}, S_{p4}
1	S_4, S_6, S_{p2}, S_{p4}	–10	S_2, S_3, S_{p2}, S_{p4}
0	S_2, S_4, S_{p2}, S_{p4}		

3. Selective harmonic elimination

In general, the number of voltage levels in a uniform step waveform for a single period is 2 $\times p+$ 1, where p is the number of voltage levels a quarter period and the number of undesired harmonic components to be eliminated is $p-1$. In the case of the proposed 21-level inverter, the number of voltage levels generated in quarter period is ten, which means the number of undesired harmonics is nine.

The 21-level inverter stepped waveform has 10 switching angles, from θ_1 to θ_{10}, and the generated voltage units are assumed to be equal. The Fourier expansion of waveform is expressed as

$$v_{out}(\theta) = A_0 + \sum_{n=1}^{\infty} A_n cos(n\theta) + B_n sin(n\theta), \tag{3}$$

where

$$A_0 = \frac{1}{2\pi}\int_0^{2\pi} f(t)dt \tag{4}$$

$$A_n = \frac{1}{\pi}\int_0^{2\pi} f(t)\sin n\omega t dt \tag{5}$$

$$B_n = \frac{1}{\pi}\int_0^{2\pi} f(t)\cos n\omega t dt \tag{6}$$

Since the generated waveform has no DC component (average value) and characterized by quarter wave and half wave symmetry, $A_0 = 0$ and the expression presented in Eq. (3) is reduced to

$$V(\theta_i) = \sum_{n=1,3,5,\ldots}^{\infty}\left[\frac{4V_{dc}}{n\pi}\sum_{i=1}^{p}\cos(n\theta_i)\right]\sin(n\theta_i), \tag{7}$$

where n is the rank of harmonics, $n = 1, 3, 5, \ldots$, V_{dc} is the value of a voltage unit, $p = (N-1)/2$ is the number of switching angles per quarter waveform, θ_i is the ith switching angle, and N is the number of the generated voltage levels per half waveform.

As mentioned before for a 21-level case, it is possible to eliminate nine undesired harmonics while maintaining the desired value of the fundamental voltage. From Eq. (7), the magnitudes of the Fourier coefficients when normalized with the respect to V_{dc}, can be expressed as follows:

$$\begin{cases} H_1 = cos\left(\theta_1\right) + \cos\left(\theta_2\right) + \ldots + \cos\left(\theta_{10}\right) m = 0 \\ H_2 = cos\left(3\theta_1\right) + \cos 3\left(\theta_2\right) + \ldots + \cos\left(3\theta_{10}\right) = 0 \\ H_3 = cos\left(5\theta_1\right) + \cos\left(5\theta_2\right) + \ldots + cos\left(5\theta_{10}\right) = 0 \\ \vdots \\ H_{10} = \cos\left(19\theta_1\right) + \cos\left(19\theta_2\right) + \ldots + \cos\left(19\theta_{10}\right) = 0 \end{cases} \tag{8}$$

In order to eliminate the 3rd, 5th, 7th, 9th, 11th, 13th, 15th, 17th, and 19th, the set of transcendental equations (8) must be solved, where $m = \left(\left(\left(N \quad - 1\right)/2\right)M/4\right)$ and M is the modulation index. The obtained angles θ_1 to θ_{10} must respect the following constraint:

$$0 < \theta_1 < \theta_2 < \theta_3 < \ldots < \theta_{10} < \frac{\pi}{2} \tag{9}$$

An objective function is an essential element in any optimization process. The objective function must be formulated in such a way that allows us to eliminate the low-order harmonics and maintain the fundamental component at a desired value; therefore it is chosen to be as follows:

$$F\left(\theta\right) = F\left(\theta_1 \ldots \theta_p\right) = \left(\sum_{i=1}^{p} \cos\left(\theta_i\right) - \frac{p\pi}{4} r\right)^2 + \sum_{n=3,5}^{2p-1} \sum_{i=1}^{p} \cos(n\theta_i) \tag{10}$$

4. Harmony search

As mentioned before, the HS is an optimization algorithm. It draws inspiration from harmony improvisation, when an artist tries to create harmony; he usually tries different combinations of music pitches on his instrument to obtain better harmony. Composing a perfect harmony is a very similar to the process of finding an optimal result for an optimization problem. HS depends on two important parameters, harmony memory considering rate ($HMCR$) and pitch adjusting rate (PAR) [13]. The algorithm is composed of three main steps: harmony memory generation, harmony improvisation, and harmony memory update [14]. In the case of SHEPWM control strategy the HS is used as an optimization tool to perform a random search for the global minima, which means forcing the objective function (10) towards a minimum value. Figure 3 demonstrates a flowchart of the HS algorithm used to solve the SHEPWM problem.

The HS algorithm begins by initializing the necessary parameters such as harmony memory size (HMS), $HMCR$, PAR, upper and lower limits ($x_{\min}$ and $x_{\max}$) and the maximum number of improvisations (NI). It should be noted that upper and the lower limits must satisfy Eq. (9). The next step is to create the initial harmony memory (HM).

The HM is a memory space in which the possible solutions can be stored. The initial HM matrix consists of many initial solution vectors randomly generated. The initial solutions are generated using the following equation:

$$x = x_{\min} + rand(x_{\max} - x_{\min}) \tag{11}$$

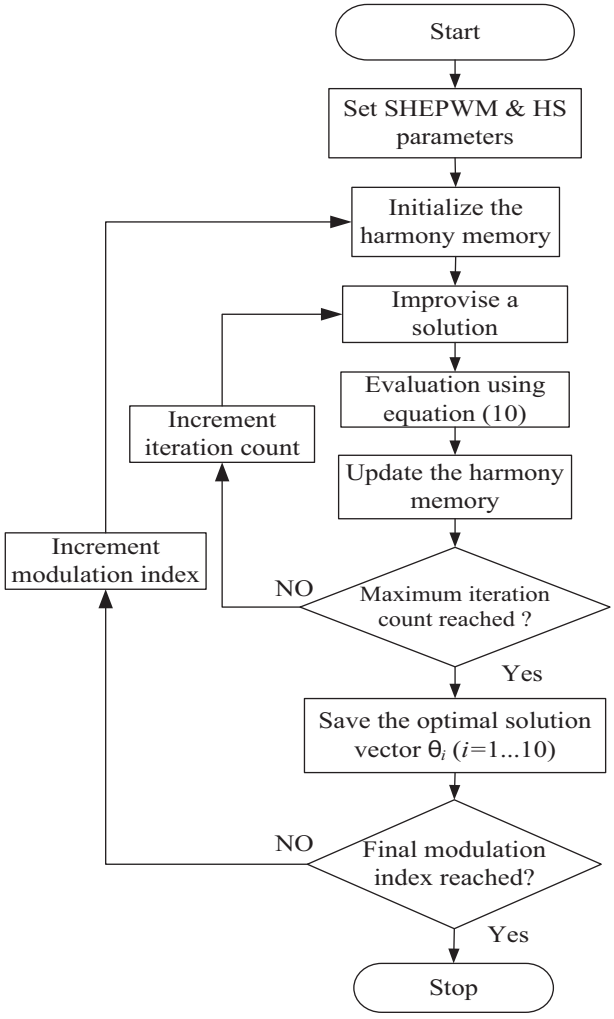

Figure 3. Harmony search (HS) flowchart for solving SHEPWM problem.

rand is a random number with a value ranging from 0 to 1 and x_{min} and x_{max} are minimum and the maximum limit values of the desired solutions. For n dimension and *HMS* size, harmony memory can be written as the following expression:

$$HM = \begin{bmatrix} x_1^1 & x_2^1 & \dots & x_n^1 \\ x_1^2 & x_2^2 & \dots & x_n^2 \\ \vdots & \vdots & \vdots & \vdots \\ x_1^{HMS} & x_2^{HMS} & \dots & x_n^{HMS} \end{bmatrix} \tag{12}$$

The next step of the algorithm is the solution improvisation. The improvisation of a new set of solutions (harmony vector) $[x_1^i x_2^i, \dots, x_n^i]$ is based on *HMCR*, *PAR*, and random selection. The *HMCR* is the selection rate of a candidate solution stored in the harmony memory (HM). The *HMCR* can have a value between 0 and 1; it is usually set between 0.7 and 0.95 in order to obtain good results [15]. ($1 - HMCR$) is the selection rate

of a random possible solution. The improvisation process can be written in the following expression:

$$x_i \leftarrow \begin{cases} x_i \in \left\{x_i^1, x_i^2, \ldots, x_i^{HMS}\right\} \text{ with probability } HMCR \\ x_i \in X_i \qquad\qquad\qquad \text{with probability } (1 - HMCR) \end{cases} \tag{13}$$

with $i \in [1, 2, \ldots, n]$ and $X_i \in [x_{min}, \ldots, x_{max}]$.

If the *HMCR* value is set to be 0.95 it means that the algorithm will choose the decision variable value from the harmony memory with a probability of 95% or a value from all the possible range (from 0 to $\pi/2$ for the SHEPWM problem) with a probability of 100%–95%. Every element of the obtained solutions is subjected to whether it should be pitch adjusted, which is determined by the *PAR*, whereas the 1 − PAR value is the rate of doing nothing. The equation below describes the adjustment operation.

$$\begin{cases} \text{Yes} \quad \text{with probability } PAR \\ \text{No} \quad \text{with probability } (1 - PAR) \end{cases} \tag{14}$$

If the pitch adjustment decision is "no" the solution x_i will not be modified; if the decision is "yes" x_i will be replaced using the following equation:

$$x_i = x_i + rand * b_w \tag{15}$$

where *rand* is a randomly generated number with a value ranging from 0 to 1 and b_w is an arbitrary distance bandwidth.

The next step of the algorithm will be the update of the *HM*. Once the improvisation is achieved, the stored *HM* elements must be updated. In this process the *HM* is updated according to the overall value of the targeted objective function presented in Eq. (10). If the new improvised harmony vector $[x_1^i x_2^i, \ldots, x_n^i]$ has a better fitness than the worst solution vector in the *HM* it will replace it [16].

The last step of the algorithm is checking the stopping condition, which in this work is the number of improvisations. If the number of improvisations reached the maximum value *(NI)*, the computation process stops. Otherwise the improvisation and the update processes are repeated.

5. ANN-based selective harmonic elimination PWM

ANNs are a very efficient tool inspired by the behavior of biological neurons; these neurons can be trained to execute a particular task by adjusting the width of the connections (also called weights) between nodes. As mentioned before, the purpose of using ANNs is to perform online SHEPWM control of the multilevel inverter. Figure 4 demonstrates the ANN structure proposed in this work. The proposed ANN structure consists of three layers: input layer, hidden layer, and output layer. The input layer is formed by a single node and takes the desired modulation index M as input. The output layer is formed by ten nodes that correspond to the switching angles.

The neural networks are trained so that the input (modulation index) leads to a desired output (switching angles). The training process requires the knowledge of a vast set of switching angles and their corresponding modulation indices. In this process, the weights (the connection between the nodes) are adjusted, based on a comparison of the output generated by the neural networks for each nodulation index and the switching angles obtained by the HS algorithm, until the network output matches the data set obtained by the HS algorithm. Although the given set of data for the ANN training is not complete and possibly not all results were obtained

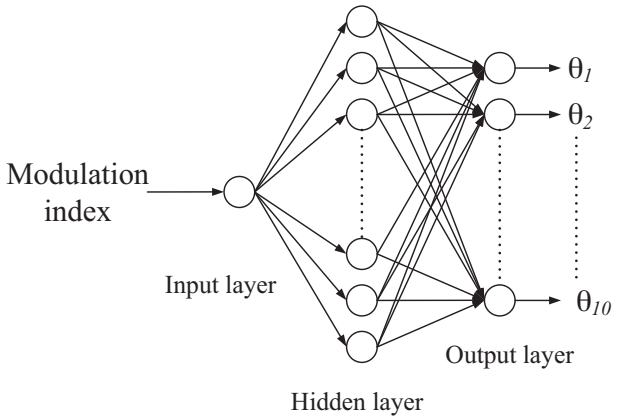

Figure 4. Artificial neural network topology.

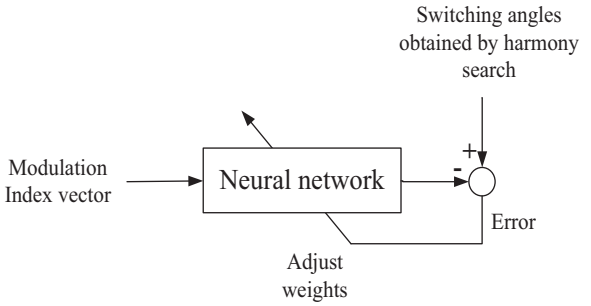

Figure 5. Artificial neural network training process.

by the HS algorithm, the ANN will be able to interpolate and extrapolate the results. Figure 5 demonstrates the training process of the ANN.

Figure 6 shows the block diagram of the proposed control scheme, the artificial neural network is activated and generates the optimal switching angles depending on the given modulation index M, SHEPWM control signals are generated by using the optimal switching angles and Table 1.

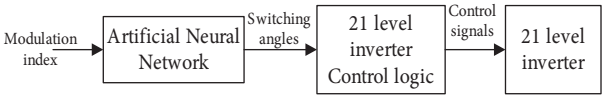

Figure 6. Block diagram of the proposed control scheme.

6. Simulation results

To test the effectiveness of the online HS SHEPWM control, a mathematical model of the proposed inverter and the control method was created using the MATLAB programming environment. Total harmonic distortion (THD) was chosen as a quality index to evaluate the quality of the generated output voltage. It can be computed using the following equation:

$$THD\% = \frac{\sqrt{\sum_{n=3}^{50} H_n^2 H_1}}{\times} 100 \tag{16}$$

The left side of Figure 7 presents the optimal switching angles (in degrees) found by the HS algorithm versus modulation index M with $M \in [0.4, 1.4]$. These angles are computed with a step size of 0.001. The solutions generated out of this range (less than 0.4 and more than 1.4) exceeded the upper limit of the constraint expressed in Eq. (9). These angles cannot be used to operate the proposed inverter and the use of these angles will lead the inverter to generate a distorted waveform. Therefore these solutions should not be taken into consideration. The right side of the same figure shows the optimal switching angles (in degrees) generated by the trained ANNs versus modulation index M. The angles are generated with a fine step size of 10^{-5}. Table 2 shows the values of the different parameters of the HS algorithm used in this simulation.

In order to confirm the validity of the proposed method, switching angles obtained from the neural networks results were applied to the mathematical model of the 21-level inverter. The fundamental frequency

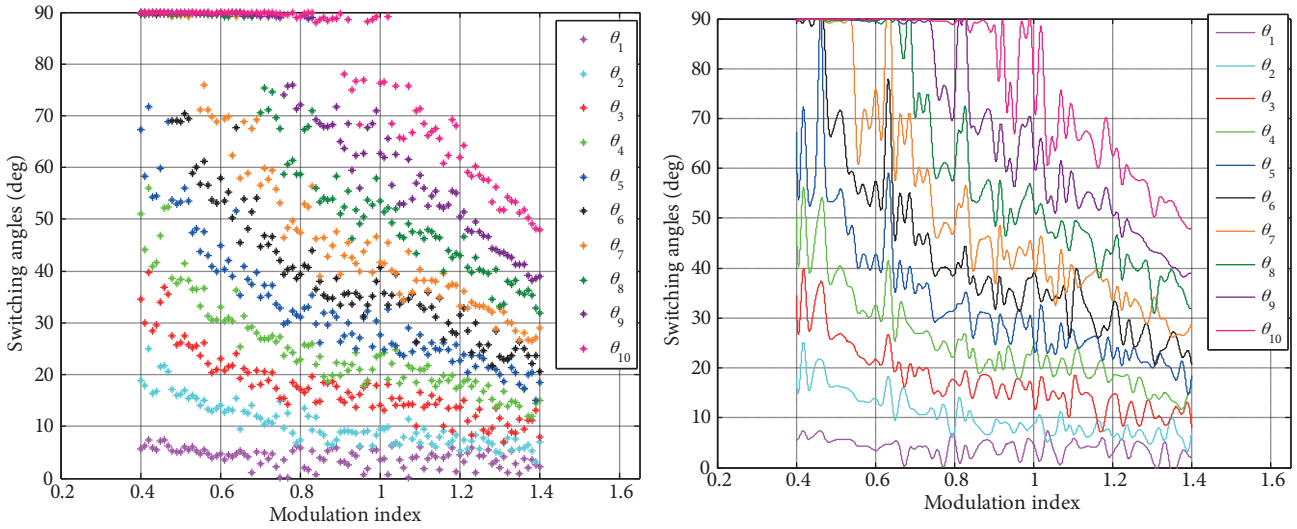

Figure 7. Switching angles versus modulation index generated by HS algorithm (left) and ANN (right).

Table 2. Harmony search parameters.

NI	1000
HMS	200
HMCR	0.95
PAR	0.1

used in this simulation is 50 Hz. The values of the DC voltage sources are chosen as follows: $V_{dc1} = V_{dc2} = V_{dc3} = 17$ V, $V_{dc4} = 119$ V. For modulation index $M = 0.975$ and $M = 0.8$, the switching angles are shown in Table 3. Figure 8 shows the voltage waveforms generated by the upper and the lower cells. It can be seen from the figure that the first cell is responsible for generating seven voltage levels, whereas the second cell is responsible of generating three voltage levels. It should be noted that the generated voltage patterns stay the same for any modulation index.

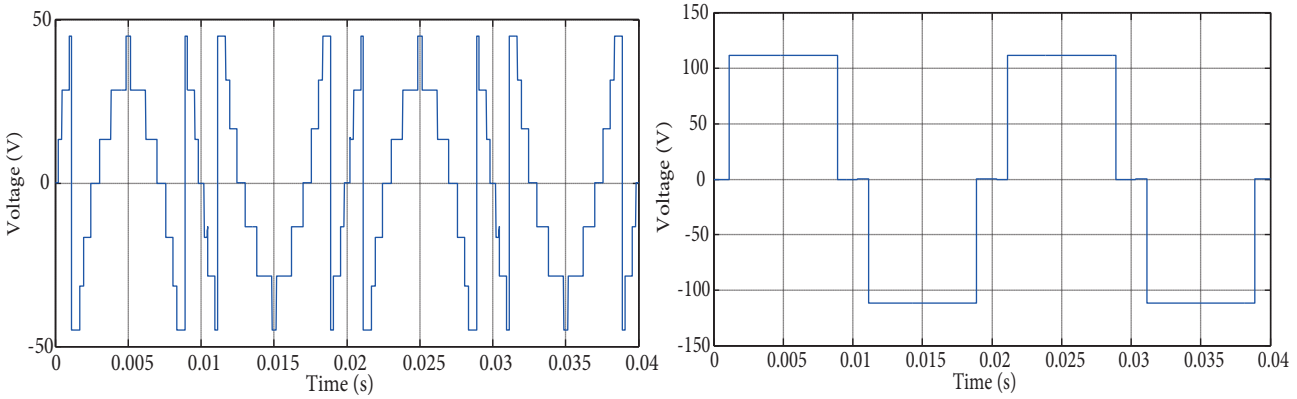

Figure 8. Voltage waveforms generated by the upper cell (left) and lower cell (right) for $M = 0.975$.

The left sides of Figures 9 and 10 show the output voltage waveform generated by the inverter for $M = 0.975$ and $M = 0.8$, respectively. The spectra of the output voltage waveforms are shown in right sides of the

Table 3. Optimal switching angles for $M = 0.975$ and $M = 0.8$.

	Angles (deg.)									
M	θ_1	θ_2	θ_3	θ_4	θ_5	θ_6	θ_7	θ_8	θ_9	θ_{10}
0.975	3.42	8.03	16.95	20.11	30.11	35.03	43.77	54.44	68.46	87.21
0.8	2.74	9.46	15.77	22.29	30.13	35.8	44.6586	53.99	67.20	82.52

same figures, and, as expected, the targeted harmonics (from the 3rd to 19th) are successfully eliminated for both modulation indices. It can be also seen that by decreasing the value of the modulation index the value of the fundamental component decreases. The total harmonic distortion was found to be $THD = 5.11\%$ for modulation index $M = 0.975$, whereas the total harmonic distortion for modulation index $M = 0.8$ was found to be $THD = 5.04\%$.

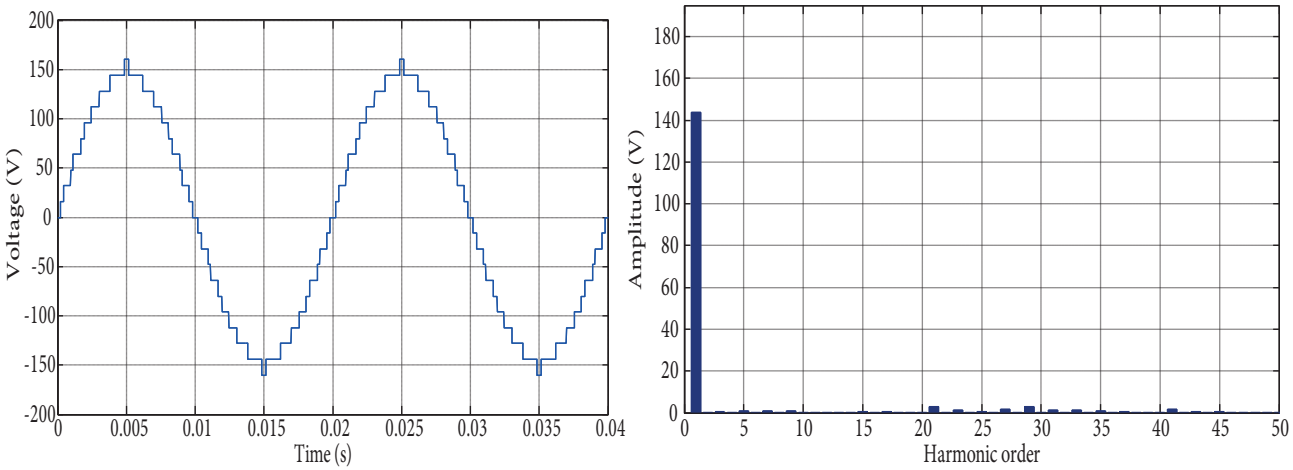

Figure 9. Voltage waveform generated by the proposed inverter and the corresponding FFT for $M = 0.975$.

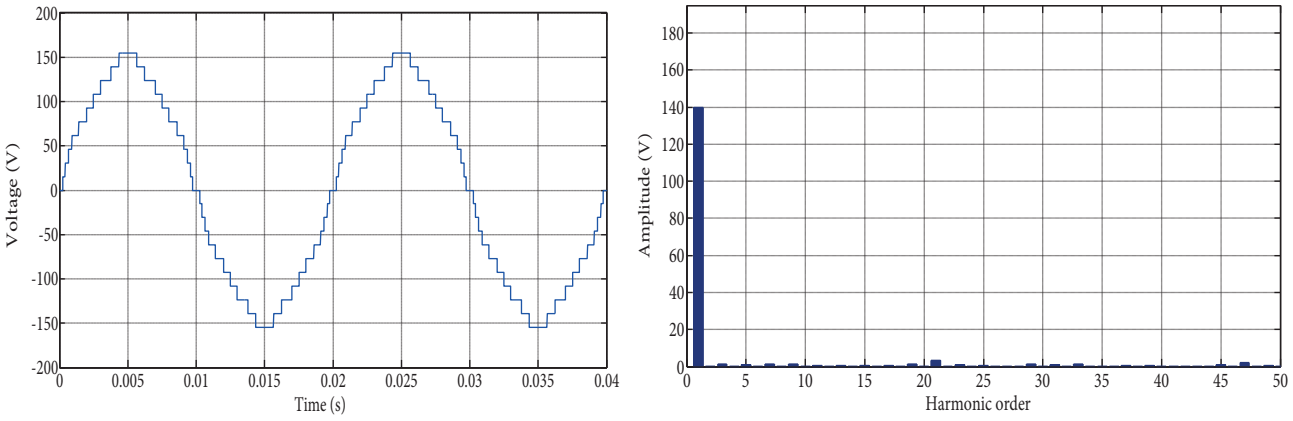

Figure 10. Voltage waveform generated by the proposed inverter and the corresponding FFT for $M = 0.8$.

7. Hardware implementation and experimental results

A small-scale laboratory prototype of a single phase 21-level inverter is built in order to verify the analytical and simulation results. H15NA50 (500 V, 15 A) n channel MOSFETs were used as the switching devices for

$S_1, S_2, S_3, S_4, S_{p1}, S_{p2}, S_{p3}$, and S_{p4}. IRG4PH30K (1200 V, 10 A) IGBT were used as used as the bidirectional switches S_5 and S_6. RHRP1560 (600 V, 15 A) fast switching diodes were used for the bidirectional switches. The laboratory prototype is shown in Figure 11. The control board consists of a STM32F407 microcontroller. The board is used to generate control signals. The gate driver board is built using TLP250 Photocouplers in order to provide electrical isolation between the control board and power circuits and also to provide proper and conditioned gating signals to the MOSFETs. An SDS1000 oscilloscope 100 MHz 500 MS/s was used to capture voltage waveforms. FFT analysis is performed by computer software connected to the oscilloscope through USB.

Figure 11. Laboratory prototype of the proposed inverter.

The experimental results of the output voltage waveforms generated by each cell are presented in Figure 12. The simulation results of 21-level output voltage patterns and their corresponding FFT presented in the previous section are experimentally validated and the results are shown in Figures 13 and 14. It can be seen that the targeted harmonics are eliminated. The total harmonic distortion of the experimental output voltage waveforms was measured and found to be $THD = 4.27\%$ for $M = 0.795$ and $THD = 4.19\%$ for $M = 0.8$. These values are very close to that found in the simulation process.

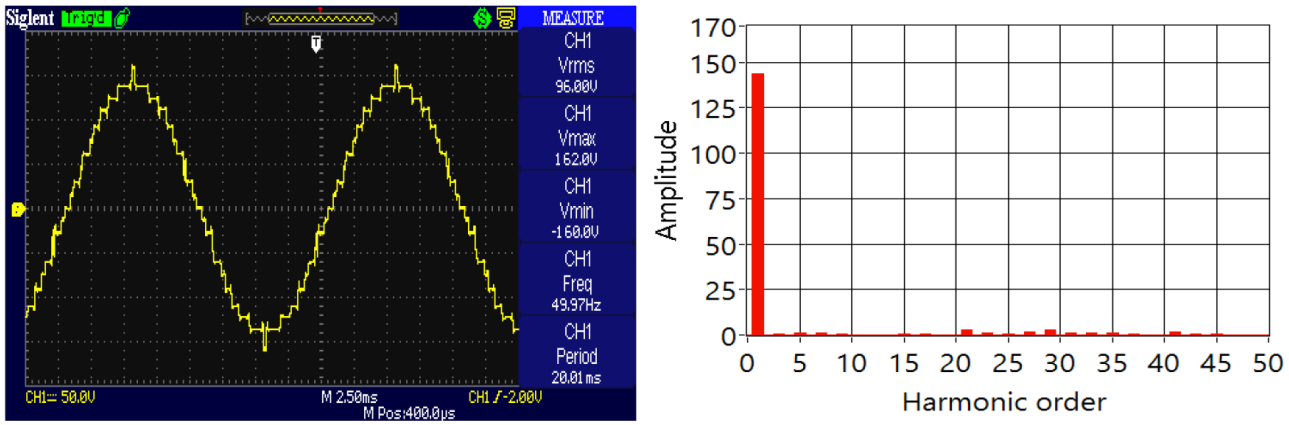

Figure 12. Voltage waveforms generated by the upper cell (left) and lower cell (right) for $M = 0.975$.

8. Conclusions

In this paper, an ANN-based SHEPWM algorithm was presented for the control of a proposed single-phase 21-level CHB inverter. The switching angles were calculated using the HS algorithm. The calculated switching angles were used for training of the ANN. The ANN-based SHEPWM algorithm was implemented on an

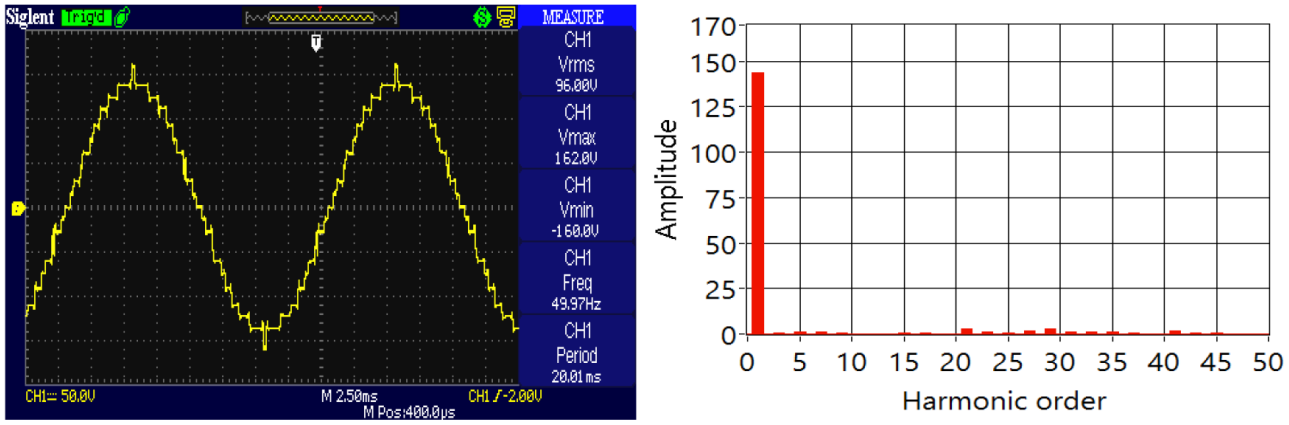

Figure 13. Harmonic spectrum of the generated voltage waveform inverter and the corresponding FFT for (experimental results) for $M = 0.975$.

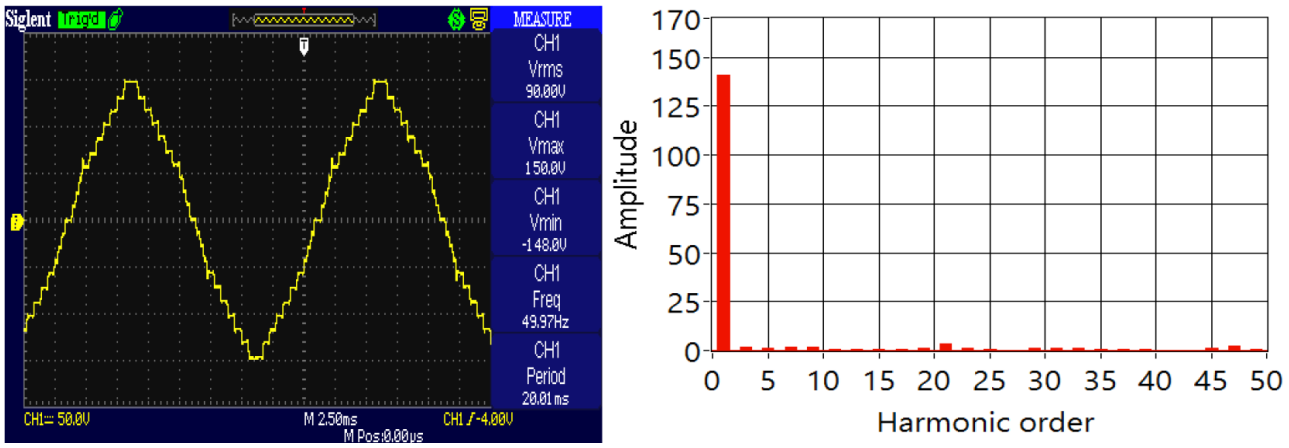

Figure 14. Harmonic spectrum of the generated voltage waveform inverter and the corresponding FFT for (experimental results) for $M = 0.8$.

STM32F407 high performance microcontroller. FFT analysis was performed on the output voltage waveform to demonstrate the performance of the ANN-HS–based SHEPWM. The experimental results showed that the 3rd, 5th, 7th, 9th, 11th, 13th, 15th, 17th, and 19th order harmonics are eliminated. The results proved that the proposed ANN-based SHPWM is suitable for switching instead of using a look-up table.

References

[1] Shalchi AR, Nazarpour D, Hosseini SH, Sabahi M. Novel topologies for symmetric, asymmetric, and cascade switched-diode multilevel converter with minimum number of power electronic components. IEEE T Ind Electron 2014; 61: 5300-5310.

[2] Patel HS, Hoft RG. Generalized techniques of harmonic elimination and voltage control in thyristor inverters: part I–harmonic elimination, IEEE T Ind Appl 1973; 9: 310-317.

[3] Gnana Sundari M, Rajaram M, Balaraman S. Application of improved firefly algorithm for programmed PWM in multilevel inverter with adjustable DC sources. Appl Soft Comput 2016; 41: 169-179.

[4] Hiendro A. Multiple Switching Patterns for SHEPWM Inverters Using Differential Evolution Algorithms. International Journal of Power Electronics and Drive Systems 2011; 1: 94-103.

[5] Taleb R, Helaimi M, Benyoucef D, Boudjema Z. Genetic algorithm application in asymmetrical 9-level inverter. International Journal of Power Electronics and Drive Systems 2016; 7: 521-530.

[6] Ganesan K, Barathi K, Chandrasekar P, Balaji D. Selective harmonic elimination of cascaded multilevel inverter using BAT algorithm. Procedia Technology 2015; 21: 651-657.

[7] Wang X, Gao XZ, Zenger K. An Introduction to Harmony Search Optimization Method. Heidelberg, Germany: Springer, 2015.

[8] Geem ZW, Kim JH, Loganathan GV. A new heuristic optimization algorithm: harmony search. Simulation 2001; 76: 60-68.

[9] Geem ZW, Kim JH, Loganathan GV. Harmony search optimization: application to pipe network design. International Journal of Modelling and Simululation 2002; 22: 125-133.

[10] Ambia MN, Hasanien HM, Al-Durra A, Muyeen SM. Harmony search algorithm-based controller parameters optimization for a distributed-generation system. IEEE T Power Deliver 2015; 30: 246-255.

[11] Maiti S, Verma V, Chakraborty C, Hori Y. An adaptive speed sensorless induction motor drive with artificial neural network for stability enhancement. IEEE T Ind Inform 2012; 8: 757-766.

[12] Filho F, Maia HZ, Mateus THA, Ozpineci B, Tolbert LM, Pinto JOP. Adaptive selective harmonic minimization based on ANNs for cascade multilevel inverters with varying DC sources. IEEE T Ind Electron 2013; 60: 1955-1962.

[13] Ayala HVH, Coelho LdS, Mariani VC, Luz MVFd, Leite JV. Harmony search approach based on Ricker map for multi-objective transformer design optimization. IEEE T Magn 2015; 51: 1-4.

[14] Hoang DC, Yadav P, Kumar R, Panda SK. Real-Time Implementation of a harmony search algorithm-based clustering protocol for energy-efficient wireless sensor networks. IEEE T Ind Inform 2014; 10: 774-783.

[15] Kim JH, Lee HM, Yoo DG. Investigating the convergence characteristics of harmony search. Adv Intel Sys Comput 2015; 382: 3-10.

[16] Askarzadeh A, Rezazadeh A. An innovative global harmony search algorithm for parameter identification of a PEM fuel cell model. IEEE T Ind Electron 2012; 59: 3473-3480.